Intact live-cell electro-launching ionization mass spectrometry: A novel method for single-cell analysis

Yunlong Shao
Beijing University of Technology
Guizhen Zhu
Beijing University of Technology
Yingyan Zhou
Beijing University of Technology
Qi Zhang
Beijing University of Technology
Yuanxing Liu
Beijing University of Technology
Huan Yao
Tsinghua University
Hanseng Zhao
Tsinghua University
Zhihui Yu
Beijing University of Technology
Xiayan Wang (xiayanwang@bjut.edu.cn)
Beijing University of Technology https://orcid.org/0000-0003-1735-0077
Sichun Zhang
Tsinghua University
Xinrong Zhang
Tsinghua University
Guangsheng Guo
Beijing University of Technology

Article

Keywords: mass spectrometry, single-cell analysis

Posted Date: March 12th, 2021

DOI: https://doi.org/10.21203/rs.3.rs-116600/v1

Abstract

Single-cell mass spectrometry (SC-MS) enables revealing cellular heterogeneity and molecular mechanism of intracellular biochemical reactions, but current SC-MS has been hindered by insufficient detection sensitivity owing to matrix interference, sample dilution, and waste of samples. Herein, we propose an intact live-cell ionization mass spectrometry (IC-ELI-MS) method based on a novel electro-launching ionization technology to greatly improve the sensitivity of single-cell detection. A narrow-bore capillary emitter is used to launch single live cells successively with almost no solvent to avoid sample dilution and matrix interference. Using IC-ELI-MS with high-speed microimaging helped achieve sample-free dilution and reveal the essence of in-source ionization of the ELI technology, thereby reducing sample waste. We applied IC-ELI-MS to multicell line single-cell metabolism fingerprint profiling, and we achieved more than 10 times higher sensitivity than that reported previously, a detection throughput of 450 cells within 20 min, 2172 cellular metabolite components were preliminarily identified. The excellent discrimination of more than 2800 single cells in various cell types shows that the method is stable, reliable, and good reproducibility. Therefore, the IC-ELI-MS technique can be used to investigate changes in single-cell metabolites under various cell conditions and disease types with high sensitivity and high throughput.

Introduction

Single-cell metabolite analysis is a promising method to reveal cellular heterogeneity from the most basic and subtle level, [1-5] especially live single-cell metabolite analysis[6], enabling to gather the most veritable biochemical information including cell differentiation and division[7-9], communication[10,11] interaction with the environment[12–14], and stress response[15]. All of this diverse information is of great significance to promote the development of cell biology and medicine, especially for facilitating cancer diagnosis, prognosis and treatment.[16] Mass spectrometry affords rapid, label-free, wide-spectrum detection, and has excellent structure qualitative capability.[13,17-19] Therefore, it is the chief method for live single-cell metabolite analysis. Currently, the majority of single-cell metabolite mass spectrometry methods utilize the electrospray ionization (ESI) technology. When droplet inkjet printing is used with conventional ESI-based methods, the separation and transportation efficiency of single cells improve to some extent, leading to improved detection throughput.[20-22] The single-cell MS technology based on probe sampling[10,23-32] using Nano-ESI enables direct sampling or extraction from single-cell samples with minimal sample preparation. Zhang's group[33] innovated the application of voltage to the MS spray to reduce the matrix interference when complex biological samples are used and extended the spray duration for single cells to qualify the sample components according to tandem MS information. Microfluidic technology-based flow cytometry combined with ESI-MS (CyESI-MS)[34-37] integrates the rapid separation, long-distance transmission, and online mass spectrometry sampling process of single-cell analysis, and it has been used to simplify the analysis system and improve the detection throughput. However, studies on single-cell ESI-MS still use the electrospray mode commonly used with a homogeneous solution model, which shows some insurmountable problems when performing the

ionization of heterogeneous single-cell samples. The use of a large amount of sheath fluid and sheath gas in the electrospray process excessively dilutes the cell sample and reduces the sample utilization. Note that thousand-fold sample dilutions can occur when the solvent used for the dissolution or extraction is in nanoliters. The sample undergoes diffusion, dilution, and ion annihilation during ionization in the atmosphere, resulting in problems such as a low sample-acquisition ratio in the MS inlet. These factors affect the sensitivity of single-cell MS detection.

Although many bioelectrospray technologies have been developed for tissue engineering and regenerative medicine[38-44], most of them did not involve MS and thus are not suitable for single-cell MS. Therefore, a novel ionization technology should be developed that can be used for complex live-cell samples to achieve high-sensitivity and high-throughput single-cell mass spectrometry.

We herein proposed an intact live-cell electro-launching ionization mass spectrometry (IC-ELI-MS) method using a narrow-bore capillary (the inner diameter (I.D.) is slightly smaller than the average diameter of the cells) to achieve efficient single-cell separation and transport to avoid sample dilution by the sheath fluid. We developed a novel ELI technology for realizing undiluted live single-cell-flow mass spectrometry. The ELI uses the thin-walled tip of a quartz tube as the outlet, which reduces the volume of the droplets formed by the combined action of the applied electric field and surface tension on the port. Consequently, the emitted cell contains only a tiny thin-layer buffer, wherein one cell acts as one droplet. The cell components are almost undiluted. Moreover, the cells remain intact and alive during the flight. Ions are generated after a charged single-cell droplet forms in the heated inlet transfer tube of the mass spectrometer, eliminating the loss of sample ions during transport through the atmospheric environment and mass spectrometer ion entrance, which is not possible in ESI. Therefore, the utilization of single-cell samples is significantly improved. Because of the abovementioned characteristics, the single-cell MS total ion chromatogram (TIC) obtained with the IC-ELI-MS for B104 cells has an average signal-to-noise (S/N) ratio of ~20:1, which is more than 10 times higher than that achieved using the existing methods of intact single-cell MS; the average cell detection throughput reaches 23 cells/min. The IC-ELI-MS method analyzed more than 300 A549 cells and obtained preliminary identification information of more than 2,000 cellular metabolites at one experiment. At least 282 cellular metabolites of them that have been reported. Additionally, more than 1000 living cells can be discriminated and completed the exact cell type attribution. using this system in one experment. Hence, it has satisfactory single-cell detection sensitivity and stability. This is a “fool-style” system with a simple structure and stable operation. It is also technically highly compatible with the commercial MS ion source equipment and has extremely low operating requirements. The wide application of this method will forcefully promote the development of single-cell metabolomics closely related to cell heterogeneity.

Results

Configuration and visual characterization of the IC-ELI-MS system

Based on our previous work on narrow-bore-capillary chromatography[45-50], we developed a single-cell MS analysis system using a novel IC-ELI mode. This analysis system focuses on realizing a high-throughput single-cell online dispersion, dilution-free MS injection, and high-sensitivity MS detection. Fig. 1 presents a structural schematic diagram of an IC-ELI-MS system. The system is simple and comprises only a narrow bifunctional capillary and an in-house-built pressurized poly(methyl methacrylate) (PMMA) chamber. The capillary has a constant I.D. throughout its entirety and a gold-sputtered thin-walled tip that can be used in the same way as a commercialized electrospray emitter is used and is compatible with all existing Nano-ESI ion sources, thereby affording convenience and facile adaptation to different conditions. A freshly prepared cell suspension was loaded into a solution vial inside the pressurized chamber and introduced into the bifunctional capillary driven by nitrogen gas for injection of cells. The cells can arrange themselves only along the capillary axis to form a single-cell flow and are launched from the constant-I.-D. thin-walled tip into the MS inlet ionizer for detection.

The necessity of each key strategy in this method was verified through a series of comparative experiments. A narrow capillary with an I.D. close to the diameter of a cell is a prerequisite for separating single cells (Supplementary Fig. 1). A capillary wall thinned by etching is necessary to generate a single-cell MS detection signal from a constant-I.D. capillary emitter (Supplementary Fig. 2). The tip with a constant I.D. has a low risk of fluid clogging, enabling a stable flow rate and a long operation life—important factors for MS detection of complex biological samples (Supplementary Fig. 3).

To investigate the operation of the system more objectively and comprehensively, an online IC-ELI-MS visualization platform was designed and built (Supplementary Fig. 4). The platform comprised a self-designed and self-manufactured ELI-MS ion source and a microscopic high-speed camera system composed of a long-distance microscope objective lens and a high-performance high-speed camera. The operation of the IC-ELI-MS system was visually recorded using this platform.

A single A549 cell moving in a narrow capillary propelled by a mobile phase was observed in real time and recorded at 10,000 frames per second (fps, Supplementary Video 1). The cell was slightly squeezed from its original sphere into a nearly cylindrical shape owing to the confinement effect when the cell passes through the narrow capillary (the I.D. was slightly smaller than the cell diameter; Fig. 2, stage a); an additional video footage of the single-cell transport inside the capillary is provided in Supplementary Video 2. In this video, the single cell appeared similar to a slug and was pushed along the capillary by the mobile phase. Once a single cell entered the capillary and began its transport, its distance from the cell in the front remained constant because the liquid is almost incompressible. Consequently, the single cells move in a single file. This result was consistent with the expected behavior of cells in narrow-bore capillaries. Thus, the use of such capillaries is one of the simplest and most reliable methods for single-cell dispersion and transport. Although narrow channels can also be built on a microfluidic chip, it is simpler and less expensive to use a capillary. Notably, even though the capillary was clogged by a few very large cells (due to cell heterogeneity), it could be flushed by applying a hydraulic pressure as low as 70–200 bar using a liquid chromatography system or simply a chromatography pump.

The ejection of an entire single cell from the constant-I.D. emitter was recorded in real time at 50,000 fps (Supplementary Video 3). The intact individual cell was ejected from the capillary tip and it carried only a tiny amount of the solvent to form the initial droplet that flew into the MS inlet. We called this initial droplet a “single-cell droplet” (Fig. 2, stage b). This unique launching phenomenon occurred at a certain voltage at the thin-walled tip of the constant-I.D. narrow capillary, which is key to resolve the dilution problem. We had also expected to achieve the same result when such a tip is used as an emitter. These results confirmed that the injection process in IC-ELI-MS was at the single-cell level instead of multiple cells simultaneously.

After synchronizing the high-speed microphotography with the single-cell MS data acquisition, three cells were successively electro-launching and recorded using the high-speed camera at 50,000 fps (at this shooting speed, the camera could record up to 5 s at the most), and their corresponding mass spectra were collected simultaneously (see Supplementary Video 4). The time interval during which the three cells participated in the electro-launching process was consistent with the retention time of the MS peaks (Supplementary Fig. 5, Supplementary Video 5). This observation proves that each signal peak in the TIC from the IC-ELI-MS system corresponded to a single cell; they do not arise from the superposition of multiple cell signals. The working mechanism of the IC-ELI-MS analysis system is shown in Fig. 2.

To further study the changes after the single-cell droplet is formed, we shifted the microscope observation field to the atmospheric section (Fig. 2, stage c) between the emitter and the MS inlet (Fig. 2, stage d); the obtained videos were combined together (Supplementary Video 6). The resulting videos directly showed that the single-cell droplet did not undergo clear droplet splitting during its flight until it entered the ion-transfer tube. To further confirm that the cells remained intact before entering the MS inlet, we placed a cover glass to obstruct and receive the single-cell droplet generated by the bifunctional capillary. The distinct stereoscopic cell profile along with good single-cell dispersion demonstrated that the cell had entered the MS inlet intact (Supplementary Fig. 6). To further verify whether IC-ELI-MS can be used for true live-cell mass spectrometry, we performed a CCK8 cell viability test experiment. For detailed experiments, see the Experimental Section and Supplementary Fig. 7 of the Supporting Information. The results show that before entering the mass spectrometer, 87.22% of the cells were still live cells. This result strongly proves that IC-ELI-MS is a live-cell analysis method.

The formation of single-cell droplets completely eliminated the dilution of single-cell samples during electro-launching. Most single-cell droplets are occupied by a cell, and the solvent is present only as an ultrathin film on the droplet surface, which reduces the dilution factor by hundreds or thousands of times compared to that achieved with traditional methods. Less solvent means less interference from impurities and less charge competition[51], which increases the S/N ratio of single-cell MS detection by one or more than one order of magnitude. Taking B104 cells as an example (Fig. 5c), the mean intensity of the cell signal peak in single-cell MS analysis of the TIC across a scan range of m/z 300–1000 was approximately 20 times that of the baseline (intensity =1×10^6) and 80 times at the highest level. The ultra-high detection sensitivity demonstrates the value of the ultra-low sample dilution characteristics of IC-ELI-MS technology.

Single-cell electro-launching ionization

We speculated that the formation of single cell electron emission ionization can be mainly attributed to the combined flow and electric fields created by the narrow-bore emitter structure with a constant I.D. and a thin-wall tip. The following experimental exploration was carried out based on this speculation.

Impact of the flow field. To evaluate the impact of the flow field in more detail, an emitter model was established, and a numerical simulation of the fluid dynamics of cell motion at the emitter outlet was performed (Fig. 3). For an emitter with a constant I.D., the smaller the I.D. of the capillary, the greater the flow rate of the mobile phase (Fig. 3a1–a3) under a constant flow rate (1 μL/min). Furthermore, the mobile phase in the high-velocity area at the emitter tip was more concentrated immediately behind the cell (Fig. 3a1–a3), suggesting that the cells ejected from the narrower emitter were subjected to a more forward thrust and were easier to rush to the front end of the liquid cone (Fig. 3b1, b2). The cell shifted downward under gravity after leaving the outlet, thus moving away from the tip of the liquid cone. Decreasing the wall thickness of the emitter throughout the column diminishes the liquid cone volume under an adequate flow rate. (The emitted cells contain very little buffer, and the cell sample is almost undiluted.) At this point, the cell had to move to the cone tip because there is no motion space left for it near the side of the liquid cone (Fig. 3b1, b2). It can be clearly demonstrated from the above simulation and deduced from the data shown in Fig. 3c, d that when the liquid cone volume generated from the emitter is smaller, the cell would contact the front side of the cone more easily. The cell, along with the mobile phase, was pulled forward by the force of the electric field after reaching the front side of the cone. As the liquid cone elongated (Fig. 3c3), the surface tension also gradually increased and applied a force to only the backside of the cell because of the flexibility of the cells to make the liquid cone contract inward until it was cut off (Fig. 3c4). At this time, a charged single-cell droplet (initial droplet) formed and was subjected to MS along the electric field line. Hence, from the perspective of fluid dynamics, to generate a single-cell droplet, a single cell must successfully reach the front side of the liqued cone. A narrow I.D. and thin emitter wall were conducive to achieving this condition. Moreover, plugging of the exit and the high back pressure at the pulled conical tip could be avoided using an emitter with a constant I.D. throughout the column to ensure long-term stability of electro-launching, which is important for high-throughput single-cell MS analysis (Fig. 3c,d, derived from Supplementary Video 7).

Impact of the electric field. To investigate the influence of the electric field on single-cell electro-launching, the launching voltage was varied in the range of 1–2 kV. Detection experiments carried out using MS can be grouped into two: one that uses a KB cell suspension as a practical sample, and the other that uses adenine aqueous solution as a standard sample; the other conditions were identical. The launching/spray currents at the corresponding voltages were recorded simultaneously for both groups of experiments. To clearly characterize the experimental results, we defined the extracted ion chromatogram (EIC) as the total intensity of the extracted ion signals during a period (area integration of peaks in extracted ion chromatography) and the TIC as the intensity of the total ion signal during a period (integration of peaks in the TIC). The detection sensitivity of samples in the same period was evaluated by EIC/TIC. KB-EIC was selected as a lipid signal with an obvious peak at m/z 785.32–790.65 in single-cell MS, and adenine-EIC

was selected at m/z 134.03–134.05, with $[M-H]^-$ m/z 134.047 (Fig. 4a). The experimental results showed a completely different relationship between the voltage and the MS signal for the KB cell suspension and adenine aqueous solution, although they have nearly overlapping current curves. The highest mass spectral signal and sample detection sensitivity were generated at 1.3–1.4 kV for the KB cell suspension; however, for the adenine aqueous solutions, the mass spectrometry signal began to increase when the spray voltage was >1.4 kV until 1.6–1.8 kV when the optimum signal was obtained. According to Taylor[52], Cloupeau and Prunet-Foch[53], Hayati[54], and Jaworek and Krupa[55], and Marginean and Vertes[56], the spray ionization effect is optimal if a homogeneous solution generates a stable Taylor cone when the spray enters the steady jet state. The adenine aqueous solution was homogeneous; thus, the voltage required for this spray system to form a steady jet should be 1.6-1.8 kV. The KB cell suspension used the same mobile phase as the adenine aqueous solution and also produced almost the same ionization current; however, it produced a completely different mass spectrum response signal, which shows that the single-cell ELI is different from the ESI mode. This phenomenon is interesting as it reveals a disadvantage of ESI-MS: the ESI technology is developed on a homogeneous solution model, and hence, it cannot cope with the characteristics of heterogeneous systems (such as cell suspensions). Hence, the IC-ELI technology is developed that can be used specifically for heterogeneous systems.

Preliminary study on the ionization mechanism of IC-ELI-MS

Using a high-speed camera, we observed that the volume of the initial droplets produced by IC-ELI remained almost constant before entering the mass spectrometer (Fig. 2, also see Supplementary Video 6 for details). This is completely different from the continuous splitting of the initial droplets into secondary droplets in ESI. We further showed the difference between the two technologies at a macro level by comparing the cell suspension and homogeneous solution during mass spectrometry injection (Supplementary Fig. 8). The cells intercepted at the entrance of the mass spectrometer still maintained a complete structure and an alive status (see Supplementary Fig. 6 and Supplementary Fig. 7). Further, most of the cell components were not ionized before entering the mass spectrometer. Hence, we believe that the ionization of single-cell components should occur in the ion-transfer tube of the mass spectrometer. Referring to similar “inlet ionization” studies[57,58], we propose the following hypotheses: After entering the MS inlet, the single-cell droplet experiences rapid boiling and an explosion in a low-pressure, high-temperature environment; then, the sample molecules rapidly moved to the gas phase and acquired random charges during the explosion. According to this assumption, the sample transferred to the gas phase and the charged proportion increase with an increase in the violent explosion.

The ionization processes taking place after a single-cell droplet enters the ion-transfer tube could not be characterized visually through a high-speed camera. Therefore, a preliminary experimental verification was carried out. We increased the temperature of the ion-transfer tube from 100 to 450 °C in stages (which is the normal adjustable parameter range of a mass spectrometer) and recorded changes in the MS signal intensity (EIC) and the MS sensitivity (EIC/TIC) for a KB cell suspension and 14 μmol/L of adenine standard (Fig. 4b). Both liquids (i.e., the KB cell suspension and the adenine standard) showed the highest mass detection sensitivity at 300 °C. However, the single-cell signal from the KB cell

suspension continuously increased under increasing temperature, whereas the signal from the adenine standard gradually decreased when the temperature was above 300 °C. Below 300 ℃, the signal intensity of both the liquids increased because regardless of whether ionization occurred out-of-source or in-source; a reasonable increase in the temperature of the ion-transfer tube promoted the desolvation of the sample and thus increased the strength of the signal arising from the sample. For a homogeneous solution, the temperature required for complete vaporization was reached readily. If the temperature continued to increase, the signal intensity decreased under the combined effects of background ion interference and space charge effect. However, for single-cell droplets with larger volumes and more complex constituents than the initial droplets produced by uniform solution electrospray, higher temperatures were needed for rapid and complete desolvation. These data corroborated our hypothesis that the cells were rapidly gasified in an ion-transfer tube to achieve ionization. From the data shown in Fig. 4b, it is clear that the single-cell MS signal intensity obtained with this system can be further improved if the temperature of the mass spectrum ion-transfer tube could be further increased to ≥400 ℃. The main characteristic of in-source ionization is that avoiding the diffusion and annihilation of sample ions in the atmosphere greatly improves the detection sensitivity and sample utilization.

Performance evaluation of IC-ELI-MS for single-cell detection

The detection throughput and sensitivity of the IC-ELI-MS system were tested using B104 cells as an example. The average single-cell detection throughput was 23 cells/min, and the TIC average S/N ratio (the baseline intensity =1×10^6) was approximately 20 times and reached 80 times at the highest scan range *m*/*z* 300-1000 (Fig. 5a–d). In addition, we analyzed over 300 A549 cells and obtained 5248 distinct signals in the scanning range *m/z* 100-1000 Da, including positive and negative modes. By matching the accurate *m/z* values obtained with the Human Metabolome Database (HMDB) with a mass tolerance of 3 ppm. A total of 2172 cellular metabolite components were preliminarily identified, of which 1343 in positive mode and 829 in negative mode. Including at least 282 cellular metabolites that have been reported, 186 and 96 in positive and negative modes, respectively (Table S1). These results may be the highest coverage in live single-cell MS experiments, demonstrating the fantastic potential of IC-ELI-MS in single-cell analysis. The cell suspension obtained from tissue digestion is usually a mixture of different cell types such as epithelial cells, glial cells, and endothelial cells. Therefore, it is necessary to investigate whether the IC-ELI-MS system can be used to identify mixed cells. The MS analysis was performed on HEK-293, B104, and CTXTNA-2 cells, as well as on a mixture of these three cell types. A total of 1280 single-cell data was collected in one experiment. We observed that these three cell types were readily discriminated, and the cell mixture was well resolved into these three cell types (Fig. 5e). Hence, the IC-ELI-MS analysis system is capable of identifying complex samples. The stability of the IC-ELI-MS system was also investigated, and the A549, KB, CTXTNA-2, B104, and HEK-293 cells were repeatedly detected by MS at different times of the day, and there were 1546 single-cell data involved (Fig. 5f). The single-cell fingerprints of all cell lines involved in the experiment obtained through IC-ELI-MS are shown in Supplementary Fig. 9.The results show that the same type of cells was clustered together on the t-

distributed stochastic neighbor embedding (t-SNE) map, indicating that the IC-ELI-MS system had good stability.

Discussion

Single-cell sequencing (SiC SEQ) technology has contributed to many great progress in the field of single-cell genomics[59–61] and transcriptomics[62,63]. However, metabolites cannot be amplified like DNA/RNA. Therefore, the development of single-cell metabolomics can only rely on detection methods with higher sensitivity. At present, single-cell metabolite MS methods suffer from several problems. First, detection sensitivity and detection coverage of existing methods are insufficient, which restrict the investigation of cell heterogeneity. Second, many single-cell MS detection methods involve complicated systems and difficult operations and have high manufacturing costs, poor stability, and difficulty in promotion. These problems arise because sample dilution, waste, and matrix interference in the electrospray process have not been resolved. In addition, these problems become more prominent when heterogeneous cell samples, such as live single cells are ionized.

We herein developed an ionization method that continuously introduces live single cells into a mass spectrometer. We achieved high sensitivity for single-cell detection, with an average S/N ratio of ~ 20:1, and sometimes even as high as 80:1, which is an order of magnitude higher than the detection sensitivity of currently high-throughput live single-cell MS methods. In addition, the average detection throughput of this method can be as high as 23 cells/min. Through the analysis of more than 300 single-cell metabolic fingerprints of A549, 2172 metabolite information was obtained. These results can be attributed to the following two characteristics: first, the narrow-bore capillary exerted a significant spatial confinement effect on the cell, and hence, can easily and reliably afford single-cell high-throughput separation along with an orderly long-distance transport, while avoiding the dilution of cell samples by sheath solution and sheath gas. Second, a novel intact live-cell electro-launching ionization is developed using a thin-walled emitter with a constant I.D. at the end of the narrow capillary. This technology can help realize single-cell mass spectrometry injection with almost no mobile phase dilution, no matrix interference, and in-source ionization, which can greatly improve the utilization of single-cell samples. Note that sample dilution, matrix interference, and sample waste are inherent defects of the ESI. In addition, a series of single-cell detection experiments with high sampling volume proved that the system has good single-cell recognition ability and stability. Hence, it is clear that this system can be used for high-throughput and high-sensitivity single-cell MS analysis.

Although the mechanism of the IC-ELI technology requires further study, it does not hinder its application. This method can be applied to all fields closely related to cell heterogeneity. For example, it can be used in the field of developmental biology to achieve a spatially resolved metabolome of cell populations in the early embryo which like the genome[64]. We expect that this method can also be applied to the high-throughput single-organelle metabolites analysis, such as nucleus and mitochondria. If this method could be extended to a broader range of heterogeneous fluid systems, direct single-particle electro-launching technology is expected to achieve high-sensitivity, high-throughput single-particle mass spectrometry,

single-particle dispersion, transfer, solvent-free capture, and provide a valuable reference for materials science, biology and other related fields.

Methods

Chemicals and Materials

Ammonium formate (LC-MS-grade), methanol (LC-MS-grade), formic acid (LC-MS-grade), adenine (MS-grade), and ammonia (Optima-grade) were purchased from Thermo Fisher Scientific (Waltham, USA). Hydrofluoric acid (40% v/v) was bought from Tianjin Fuchen Chemical Reagent Factory (Tianjin, China). Ultrapure water (resistance = 18.2 $M\Omega \cdot cm^{-1}$) was prepared using a GenPure UV/UF water purification system (Thermo Fisher Scientific, USA). Fused-silica capillary (16 μm I.D., 360 μm O.D.) was acquired from Yongnian Ruifeng Chromatographic Device Co., Ltd (Hebei, China). Nitrogen (≥99.9999%) was obtained from Beijing Tianli Renhe Gas Co., Ltd (Beijing, China).

A549, 293, KB, B104, and CPXTNA-2 cells were obtained from the Cell Resource Center of the Institute of Basic Medical Sciences, Chinese Academy of Medical Sciences (Beijing, China). Dulbecco's Modified Eagle Medium (DMEM), trypsin-ethylenediaminetetraacetic acid (0.25%, trypsin-EDTA), penicillin-streptomycin (100 $U \cdot mL^{-1}$), dimethyl sulfoxide (99.5%, DMSO), fetal bovine serum (FBS), and phosphate buffer solution (PBS) were purchased from Thermo Fisher Gibco (Waltham, USA).

Fabrication of narrow-bore bifunctional capillaries

A 30-cm-long capillary was cut, and its one end was etched using the wet etching protocols established previously by our research group to obtain a tip. [49, 65] The capillary tip was surface-cleaned with plasma for 15 min using a plasma cleaner. Then, chromium was sputtered (working air: argon; power: 5 W; sputtering time: 3 min) using a low-temperature magnetic sputtering instrument (JS3S-80G, Beijing Jinshengweina Technology Co., Ltd.), followed by the sputtering of gold (working air: argon; power: 5 W; sputtering time: 6 min). Finally, the capillary tip was stored in an airtight, dust-free environment for future use. The chromium layer can increase the adhesion of the conductive coating on the surface of the silica-fused capillary, the stability of the conductive layer, and can extend the operation life of the emitter (see Supplementary Fig. 10).

Preparation of cell suspensions

Cells grown to a coverage of 80%-90% were trypsinized using trypsin-EDTA (0.25%). The trypsinization process was terminated using a fresh culture medium. Then, the trypsin-EDTA-containing residual culture medium was removed by centrifugation (1200 rpm, 3 min) and the obtained cells were resuspended into the DMEM culture medium. Appropriate volume cell suspensions were centrifuged at 2000 rpm for 3 min to remove the culture medium and cleaned with 150 mmol/L of ammonium formate (pH = 7.4). Finally, the cells were resuspended into 40 mmol/L of ammonium formate aqueous solution.

Verification of cell viability using CCK8

A549 was selected after subculture for 2 days for the experiment. A549 that passed the IC-ELI-MS sampling device in front of the ion inlet of the mass spectrometer was selected as the experimental group (using a centrifuge tube containing a culture medium to receive the cells). The cells that have undergone the IC-ELI-MS sample preparation process were collected as the control group (the cells were immediately centrifuged and resuspended in the medium after the sample preparation process was completed), and the cells without any treatment were used as the blank group. Next, 5000 cells/well were inoculated on a 96-well culture plate. Each sample was set with three replicate wells, to which 10 μL of CCK8 reaction solution was directly added after the inoculation, and the cells were incubated for 30 min at 37 ℃ in the dark. A microplate reader (SpectraMax M4, AD, USA) was used to measure the absorbance at a wavelength of 450 nm.

Single-cell mass spectrometry

All the mass spectra data were acquired on an LTQ Orbitrap XL mass spectrometer (Thermo Scientific San Jose, CA, USA). The MS parameters were set as follows: The voltage was controlled from -1.3 to -1.4 kV using a spray current at 0.2–0.7 μA under negative-ion full MS scan mode, although slight differences were observed according to specific experimental conditions. The following conditions were used: MS inlet temperature = 320 ℃, resolution = 30000, maximum inject time = 20 ms, AGC target = 8×10^4, scanning range = 100–1000 Du or 300–1000 Du.

Data analysis

Raw data processing was performed on a metabolite data analysis platform developed by our group[3]. The source code of the MATLAB software used is https://github.com/HansenZhao/PeakPicker. Ions with a signal-to-noise ratio (S/N ratio) of >3 and an occurrence frequency of >10% in all cell events were considered as the detected signals. Lipid metabolites were the major constituents of cell membranes, and hence, they could be used as a reliable reference for the differentiation of cell profiles and the electro-launching ionization of sensitive substances. Nonlinear reduction of complex metabolic data sets using a machine learning method is based on the t-distributed stochastic neighbor embedding (t-SNE), which could qualitatively discriminate subtle groups and visualize the difference in the two-dimensional plane.

More information about single-cell matching could be obtained by referring to various databases available online, including Human Metabolome Database (http://www.hmdb.ca/)

Numerical simulation of hydrodynamics in cell motion process at the exit of the narrow capillary emitter with constant inner diameter

Model settings. To simulate the flow of particles in a multiphase system flow, the Eulerian model was used along with the dynamic mesh method for the dynamic simulation of particle motion. A velocity

distribution diagram of the particle at the exit of the emitter was obtained. The Dynamic Mesh Zones software was used for the calculation.

Border conditions. The liquid phase system comprised of water. The flow rate was 1 μL/min, and the I.D.s of the emitters were 16, 50, and 100 μm. At the pressure exit, a 15-μm-diameter rigid particle with a density of 1552 kg/m^3, the same as the cell density, was present. No voltage was applied to the simulation system. Opening the gravity tab and a comprehensive motion trajectory was obtained. The numerical simulation result showed that as the diameter of the capillary increased, the exit velocity of the particle and the shear stress of the wall surface on the particle significantly reduced（Table S2）.

Declarations

Acknowledgments

This work was supported by the National Natural Science Foundation of China (Nos. 21625501, 21527808, 21936001), the Beijing Outstanding Young Scientist Program (BJJWZYJH01201910005017), and the Beijing Municipal High Level Innovative Team Building Program (IDHT20180504).

Author contributions

X.W., S.Z., and G.G. conceived the project. X.W. and Y.S. designed the experiment. Y.S. modified the instrument and designed the machine under the guidance of X.W., X.Z., S.Z., Z.Y., and L.L., Q.Z., Y.S. and Y.Z. performed the high-speed photography and the corresponding data analysis. Y.S. and G.Z. prepared the materials and performed the mass spectrometry detection. H.Y., H.Z. and Y.L. performed the data analysis. Y.S. designed and performed the simulations under the guidance of X.W., Y.S. and Y.Z. wrote the manuscript. All the authors discussed the results and commented on the manuscript.

Competing interests

The authors declare no competing interests.

Data availability

The data that support the findings of this study are available on reasonable request from the corresponding author. The data are not publicly available because they contain information that might compromise the privacy of the research participants.

Code availability

The custom MATLAB code used for the analyses is available upon request from the corresponding author.

References

1. Chen, H. Y. Bioanalysis in single cells: Current advances and challenges. *China-Chem.* **63,** 564-588 (2020).
2. Ibáñez, A. J., et al. Mass spectrometry-based metabolomics of single yeast cells. *Natl. Acad. Sci. U.S.A.* **110**, 8790-8794 (2013).
3. Pareek, V., Tian, H., Winograd, N., Benkovic, S. J. & Tian, H. Metabolomics and mass spectrometry imaging reveal channeled de novo purine synthesis in cells. *Science* **368**, 283-290 (2020).
4. Onjiko, R. M., Moody, S. A. & Nemes, P. Single-cell mass spectrometry reveals small molecules that affect cell fates in the 16-cell embryo. *Natl. Acad. Sci. U.S.A.* **112**, 6545-6550 (2015).
5. Fessenden, M. Metabolomics: Small molecules, single cells. *Nature* **540**, 153-155 (2016).
6. Earl, D. C., et al. Discovery of human cell selective effector molecules using single cell multiplexed activity metabolomics. *Commun.* **9**, 39 (2018).
7. Xu, X., et al. Microfluidic single-cell omics analysis. *Small* **16**, 1903905 (2020).
8. Oginuma, M. et al. Intracellular pH controls WNT downstream of glycolysis in amniote embryos. *Nature* **584**, 98-101 (2020).
9. Trefely, S. & Wellen, K. E., Metabolite regulates differentiation. *Science* **360**, 6389 (2018).
10. Artyomov, M. N. & Van den Bossche, J., Immuno-metabolism in the single-cell Era. *Cell Metab.* doi: 10.1016/j.cmet.2020.09.013 (2020).
11. Hartmann, F. J., et al. Single-cell metabolic profiling of human cytotoxic T cells. *Biotechnol.* doi:10.1038/s41587-020-0651-8 (2020).
12. Zhu, H. Y., et al. Moderate UV exposure enhances learning and memory by promoting a novel glutamate biosynthetic pathway in the brain. *Cell* **173**, 1716-1727 (2018).
13. Zhang, L. W. & Vertes, A., Single-cell mass spectrometry approaches to explore cellular heterogeneity. *Chem. Int. Ed.* **57**, 4466-4477(2018),
14. Xue, M., et al. Chemical methods for the simultaneous quantitation of metabolites and proteins from single cells. *Am. Chem. Soc.* **137**, 4066-4069 (2015).
15. Hines, P. J., Metabolite channeling by a dynamic metabolon, *Science* **354**, 843 (2016).
16. Zenobi, R., Single-cell metabolomics: analytical and biological perspectives. *Science* **342**, 1243259 (2013).
17. Comi, T. J., Do, T. D., Rubakhin, S. S. & Sweedler, J. V. Categorizing cells on the basis of their chemical profiles: progress in single-cell mass spectrometry. *Am. Chem. Soc.* **139**, 3920-3929 (2017).
18. Shrestha, B., Single-cell metabolomics by mass spectrometry*, Single Cell Metabolism* 1-8, (Humana Press 2020).
19. Duncan, K. D., Fyrestam J. & Lanekoff I. Advances in mass spectrometry based single-cell metabolomics. *Analyst* **144**, 782-793 (2019).
20. Chen, F., et al. Single-cell analysis using drop-on-demand inkjet printing and probe electrospray ionization mass spectrometry. *Chem.* **88**, 4354-360 (2016).

21. Zhang, W., et al. Inkjet printing based droplet generation for integrated online digital polymerase chain reaction. *Chem.* **90**, 5329-5334 (2018).
22. Cahill, J. F., Riba, J. & Kertesz, V. Rapid, untargeted chemical profiling of single cells in their native environment. *Chem.* **91**, 6118-6126 (2019).
23. Wei, Z. W., et al. Pulsed direct current electrospray: Enabling systematic analysis of small volume sample by boosting sample economy. *Chem.* **87**, 11242-11248 (2015).
24. Tsuyama, N., Mizuno, H., Tokunaga, E. & Masujima, T. Live single-cell molecular analysis by video-mass spectrometry. *Sci.* **24**, 559-561 (2008).
25. Gholipour, Y., Erra-Balsells, R., Hiraoka, K. & Nonami, H. Living cell manipulation, manageable sampling, and shotgun picoliter electrospray mass spectrometry for profiling metabolites. *Biochem.* **433**, 70-78 (2013).
26. Pan, N., et al. The single-probe: A miniaturized multifunctional device for single cell mass spectrometry analysis. *Chem.* **86**, 9376-9380 (2014).
27. Liu, R., Pan, N., Zhu, Y. & Yang, Z. T-probe: an integrated microscale device for online in situ single cell analysis and metabolic profiling using mass spectrometry. *Chem.* **90**, 11078-11085 (2018).
28. Shao, Y., Zhou, Y., Wu, Y., Zhang, Q., Yu, Z., Guo, G. & Wang, X. Controllable fabrication of pico/femtoliter pipette sampling probes and visual sample volume determination. *Talanta*, **218,** 121096 (2020).
29. Zhang, X. C., et al. Combination of droplet extraction and pico-ESI-MS allows the identification of metabolites from single cancer cells. *Chem.* **90**, 9897-9903 (2018).
30. Wang, R., et al. Metabolic discrimination of breast cancer subtypes at the single-cell level by multiple microextraction coupled with mass spectrometry. *Chem.* **91**, 3667-3674 (2019).
31. Feng, J., et al. Quantitation of glucose-phosphate in single cells by microwell-based nanoliter droplet microextraction and mass spectrometry. *Chem.* **91**, 5613-5620 (2019).
32. Guillaume-Gentil, O., et al. Single-cell mass spectrometry of metabolites extracted from live cells by fluidic force microscopy. *Chem.* **89**, 5017-5023 (2017).
33. Wei, Z. W., et al. Rapid removal of matrices from small-volume samples by step-voltage nanoelectrospray. *Chem. Int. Ed.* **52**, 11025-11028 (2013).
34. Huang, Q., Mao, S., Khan, M., Zhou, L. & Lin, J. M. Dean flow assisted cell ordering system for lipid profiling in single-cells using mass spectrometry. *Commun.* **54**, 2595-2598 (2018).
35. Yao, H., et al. Label-free mass cytometry for unveiling cellular metabolic Heterogeneity. *Chem.* **91**, 9777-9783 (2019).
36. Zhu, Y., Liu, R. & Yang, Z. Redesigning the T-probe for mass spectrometry analysis of online lysis of non-adherent single cells. *Chim. Acta* **1084**, 53-59 (2019).
37. Xu, S., Liu, M., Bai, Y. & Liu, H., Multi-dimensional organic mass cytometry: Simultaneous analysis of proteins and metabolites on single cells. *Chem. Int. Ed.* doi: 10.1002/anie.202009682 (2020).

38. Jayasinghe, S. N., Eagles, P. A. M. & Qureshi, A. N. Electric field driven jetting: An emerging approach for processing living cells. *J.* **1**, 86-94 (2006).
39. Jayasinghe, S. N., Qureshi, A. N. & Eagles, P. A. M. Electrohydrodynamic jet processing: An advanced electric-field-driven jetting phenomenon for processing living cells. *Small* **2**, 216-219 (2006).
40. Eagles, P. A. M., Qureshi, A. N. & Jayasinghe, S. N. Electrohydrodynamic jetting of mouse neuronal cells. *J.* **394**, 375-378 (2006).
41. Odenwälder, P. K., Irvine, S., McEwan, J. R. & Jayasinghe, S. N. Bio-electrosprays: A novel electrified jetting methodology for the safe handling and deployment of primary living organisms. *J.* **2**, 622-630 (2007).
42. Sahoo, S., Lee, W. C., Goh, J. C. H. & Toh, S. L. Bio-electrospraying: A potentially safe technique for delivering progenitor cells. *Bioeng.* **106**, 690-698 (2010).
43. Braghirolli, D. I., et al. Bio-electrospraying of human mesenchymal stem cells: An alternative for tissue engineering. *Biomicrofluidics* **7**, 044130 (2013).
44. Maurmann, N., Sperling, L. E. & Pranke, P. *Cutting-Edge Enabling Technologies for Regenerative Medicine* 79-100 (Springer Press, Singapore, 2018).
45. Wang, X., et al. Free solution hydrodynamic separation of DNA fragments from 75 to 106 000 base pairs in a single run. *Am. Chem. Soc.* **132**, 40-41 (2010).
46. Wang, X., et al. Pressure-induced transport of DNA confined in narrow capillary channels. *Am. Chem. Soc.* **134**, 7400-7405 (2012).
47. Liu, L., et al. High-resolution hydrodynamic chromatographic separation of large DNA using narrow, bare open capillaries: A rapid and economical alternative technology to pulsed-field gel electrophoresis? *Chem.* **86**, 729-736 (2014).
48. Liu, L., Veerappan, V., Bian, Y., Guo, G. & Wang, X. Influence of elution conditions on DNA transport behavior in free solution by hydrodynamic chromatography. *China Chem.* **58**, 1605-1611 (2015).
49. Li, R. N., Shao, Y. L., Yu, Y. M., Wang, X. Y. & Guo, G. S. Pico-HPLC system integrating an equal inner diameter femtopipette into a 900 nm ID porous layer open tubular column. *Commun.* **53**, 4104-4107 (2017).
50. Zhang, W., et al. Visual and real-time imaging focusing for highly sensitive laser-induced fluorescence detection at yoctomole levels in nanocapillaries. *Commun.* https://doi.org/10.1039/C9CC09594B (2020).
51. Susa, A. C., Xia, Z. & Williams, E. R. Small emitter tips for native mass spectrometry of proteins and protein complexes from nonvolatile buffers that mimic the intracellular environment. *Chem.* **89**, 3116-3122 (2017).
52. Taylor, G. The force exerted by an electric field on a long cylindrical conductor. *Roy. Soc. Lond. A Mat.* **291**, 145-158 (1966).
53. Cloupeau, M. & Prunet-Foch, B. Electrohydrodynamic spraying functioning modes: A critical review. *Aerosol Sci.* **25**, 1021-1036 (1994).

54. Hayati, I., Bailey, A. I. & Tadros, T. F. Mechanism of stable jet formation in electrohydrodynamic atomization. *Nature* **319**, 41-43 (1986).
55. Jaworek, A. & Krupa, A. Classification of the modes of EHD spraying. *Aerosol Sci.* **30**, 873-893 (1999).
56. Nemes, P., Marginean, I., & Vertes, A. Spraying mode effect on droplet formation and ion chemistry in electrosprays. *Chem.* **79**, 3105-3116 (2007).
57. McEwen, C. N., Pagnotti, V. S., Inutan, E. D. & Trimpin, S. New paradigm in ionization: Multiply charged ion formation from a solid matrix without a laser or voltage. *Chem.* **82**, 9164-9168 (2010).
58. Pagnotti, V. S., Chubatyi, N. D. & McEwen, C. N. Solvent assisted inlet ionization: An ultrasensitive new liquid introduction ionization method for mass spectrometry. *Chem.* **83**, 3981-3985 (2011).
59. Lareau, C. A. et al, Massively parallel single-cell mitochondrial DNA genotyping and chromatin profiling. *Biotechnol.* doi: 10.1038/s41587-020-0645-6 (2020)..
60. Lareau, C. A. et al, Droplet-based combinatorial indexing for massive-scale single-cell chromatin accessibility. *Biotechnol.* **37**, 916-924 (2019).
61. Lan, F., Demaree, B., Ahmed, N. & Abate, A. R., Single-cell genome sequencing at ultra-high-throughput with microfluidic droplet barcoding. *Biotechnol.* **35**, 640-646 (2017).
62. Rizvi, A. H. et al, Single-cell topological RNA-seq analysis reveals insights into cellular differentiation and development. *Biotechnol.* **35**, 551-560 (2017).
63. Faridani, O. R. et al., Single-cell sequencing of the small-RNA transcriptome. *Biotechnol.* **34**, 1264-1266 (2016).
64. Peng, G. et al. Molecular architecture of lineage allocation and tissue organization in early mouse embryo. *Nature* **572**, 528-532 (2019).
65. Wang, X. Y. , Shao, Y. L. , Wang, L. & Gang, G. S. Dual-functional equal-inner-diameter skin flow mass spectrum spray needle and preparation method thereof. CHN patent ZL 201610125665.4 (2016)

Figures

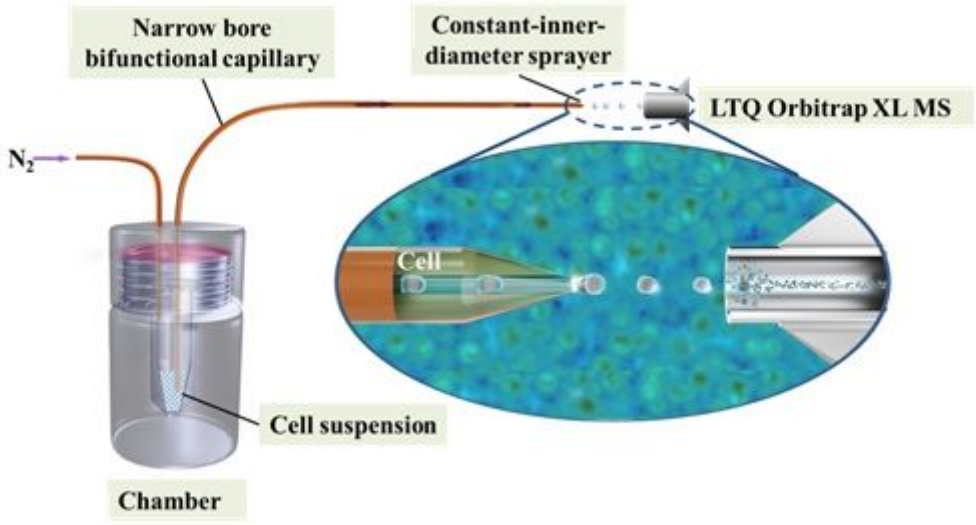

Figure 1

Schematic illustration of the IC-ELI-MS system.

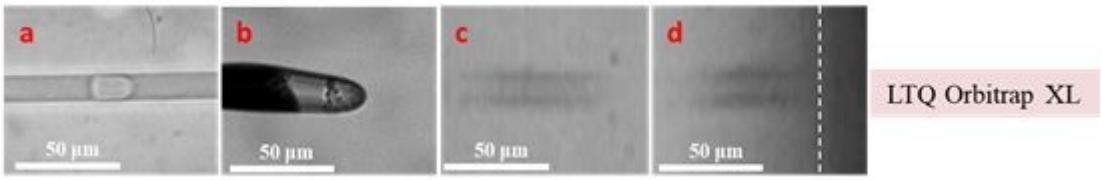

Figure 2

Electro-launching process in the IC-ELI-MS system. Illustration (top) and corresponding imaging (bottom) of the stages of electro-launching of a single cell: a. Motion of a single cell through a narrow capillary. b. The cell reaches the front of the liquid cone. c and d. The single-cell droplet flows through the atmosphere and enters the MS ion-transfer tube. HV: High voltage.

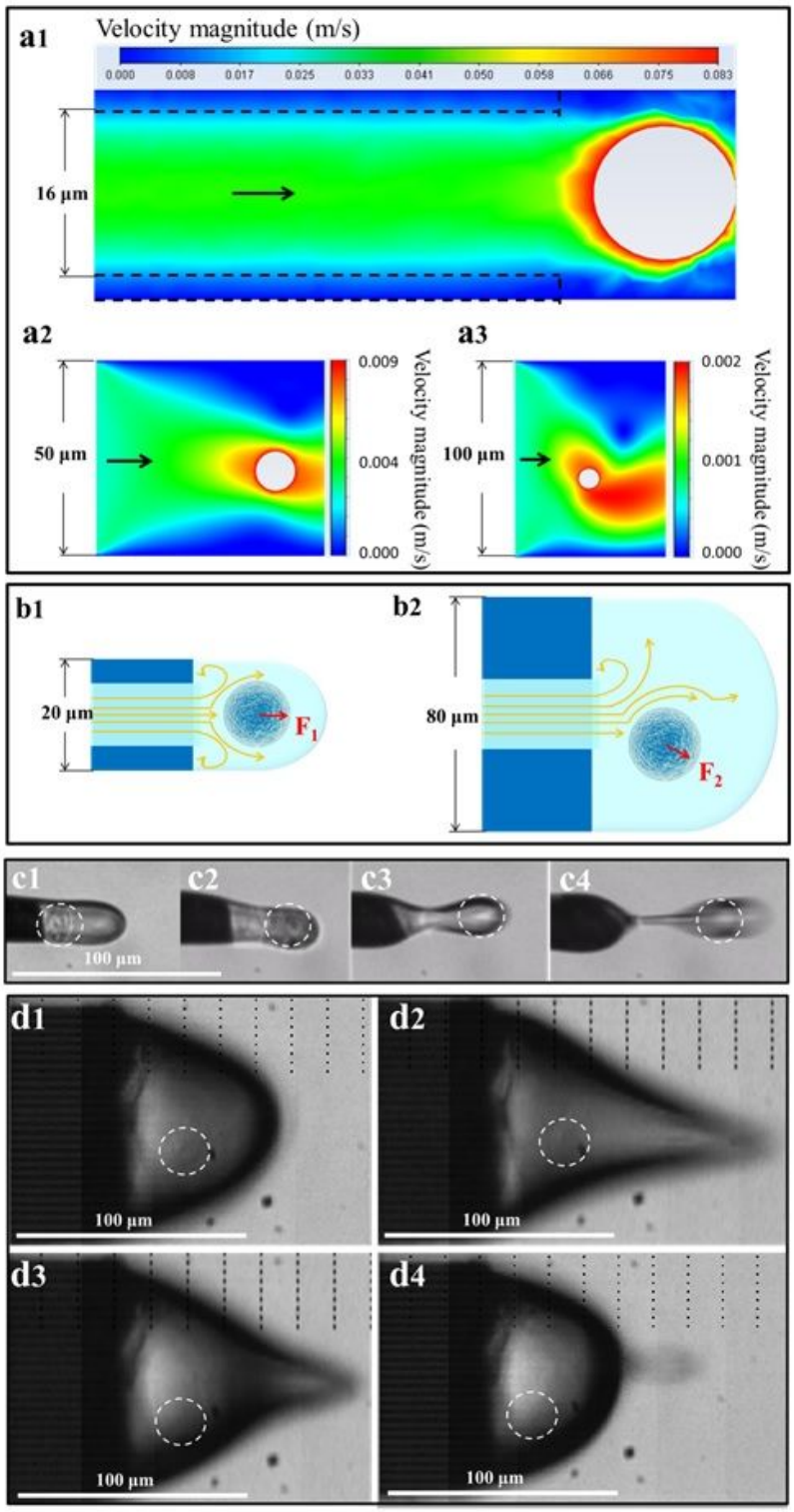

Figure 3

Flow field generated by the single-cell electro-launching. a. Velocity distribution diagram of the liquid surrounding a cell near the outlet of emitters with the I.D.s of 16 μm (a1), 50 μm (a2), and 100 μm (a3). b. Stress diagram of the liquid associated with a cell at the outlet of emitters with the O.D.s of 20 μm (b1) and 80 μm (b2). c and d. High-speed screenshots of one launching circle when the O.D. of the emitter was

20 μm (c) and 80 μm (d). The white circles marked in c1–c4 and d1–d4 represent the presence of a real single cell.

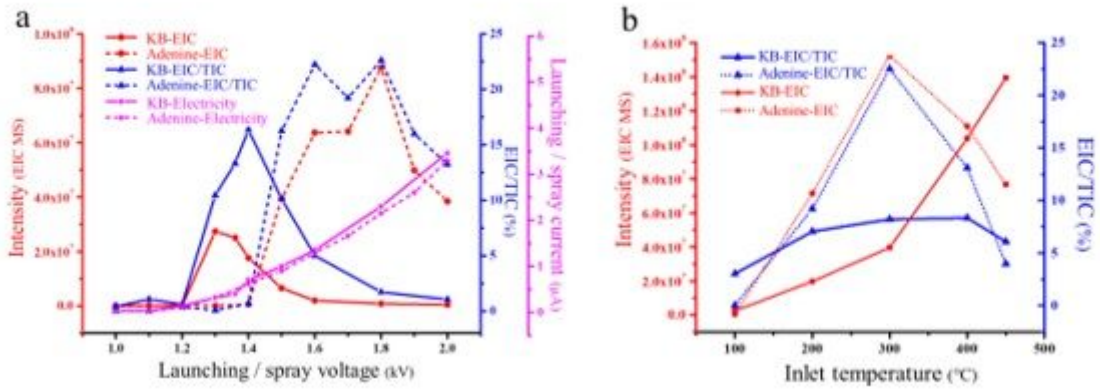

Figure 4

Difference between single-cell electro-launching ionization and solution electrospray ionization. a. Influence of the launching/spray voltage (1–2 kV) on the single-cell/adenine MS signal intensity in negative-ion mode. b. Influence of temperature of the ion-transfer capillary entrance (100, 200, 300, 400, and 450 °C) on the single-cell/adenine MS signal intensity. KB-EIC: EIC of the lipid ions at m/z 785.32–790.65 in KB cells; Adenine-EIC: EIC of adenine at m/z 134.03–134.05, ([M−H]− m/z 134.047); KB-TIC: Total ion intensity from KB cells; Adenine-TIC: Total ion intensity of adenine; KB-Electricity: Launching current of a KB cell suspension; Adenine-Electricity: Spray current of an adenine aqueous solution.

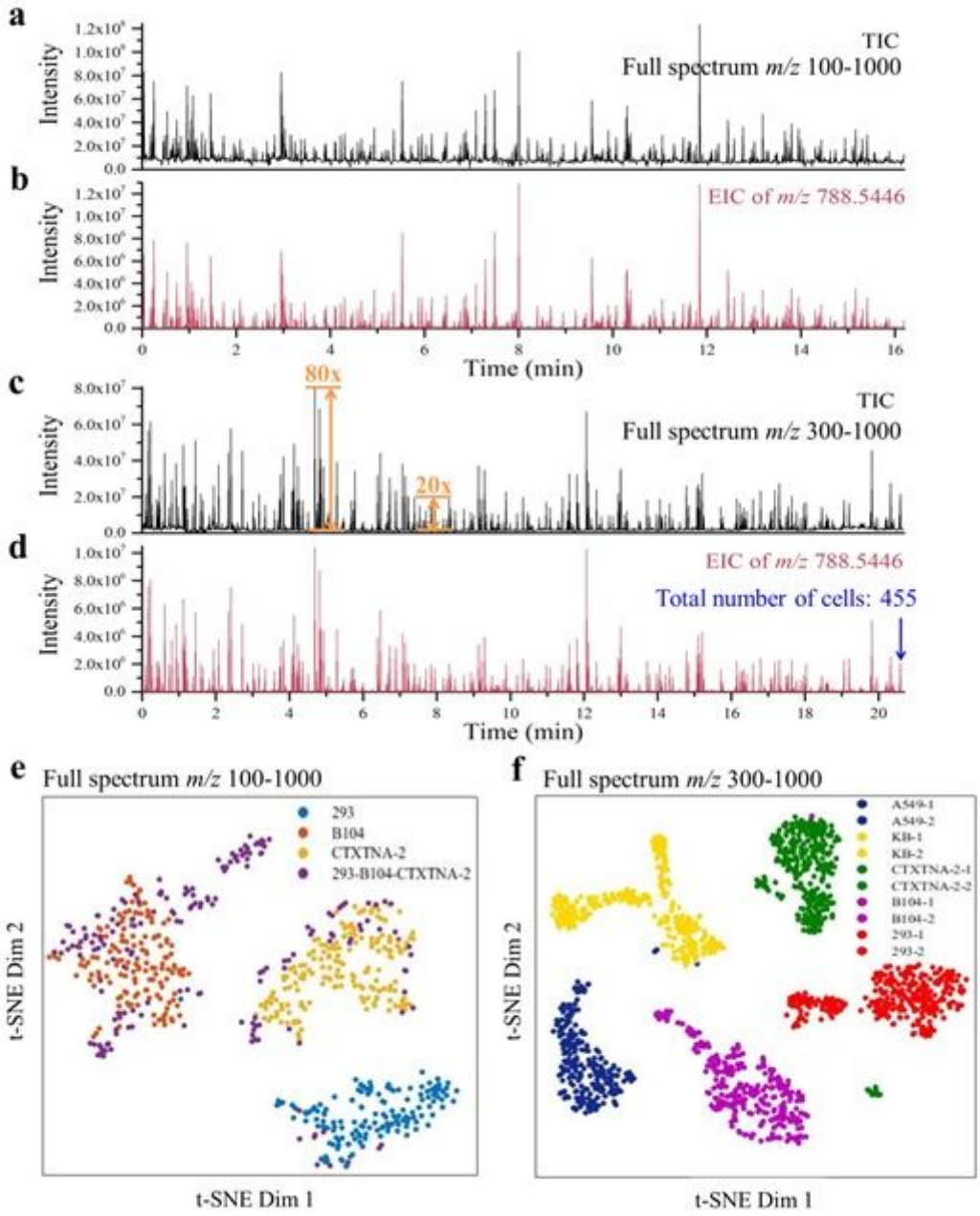

Figure 5

Performance of the IC-ELI-MS method for single-cell detection. a, TIC of B104 cells; full scan range, m/z 100–1000. b and d. EIC of m/z 788.5446 from a and c, respectively. c, TIC of B104 cells; full scan range, m/z 300–1000. The boundaries between each population are obvious in e and f. e. The t-SNE map of HEK-293, B104, and CTXTNA-2 cells and a mixture of these three cell types. f. t-SNE map of A549, KB, CTXTNA-2, B104, and HEK-293 cells based on their mass spectra measured at different time periods. (“-1” were measured at a.m., “-2” at p.m.).

Supplementary Files

This is a list of supplementary files associated with this preprint. Click to download.

- Video1.avi
- Video2.avi
- Video3.avi
- Video4.avi
- Video5.avi
- Video6.avi
- Video7.avi
- Video8.avi
- Supportinginformation1.pdf
- Supportinginformation2.pdf